The Intercalibration of Geostationary Visible Imagers Using Operational Hyperspectral SCIAMACHY Radiances

David R. Doelling, Benjamin R. Scarino, Daniel Morstad, Arun Gopalan, Rajendra Bhatt, Constantine Lukashin, and Patrick Minnis

***Abstract*—Spectral band differences between sensors can complicate the process of intercalibration of a visible sensor against a reference sensor. This can be best addressed by using a hyperspectral reference sensor whenever possible because they can be used to accurately mitigate the band differences. This paper demonstrates the feasibility of using operational Scanning Imaging Absorption Spectrometer for Atmospheric Cartography (SCIAMACHY) large-footprint hyperspectral radiances to calibrate geostationary Earth-observing (GEO) sensors. Near simultaneous nadir overpass measurements were used to compare the temporal calibration of SCIAMACHY with Aqua Moderate Resolution Imaging Spectroradiometer band radiances, which were found to be consistent to within 0.44% over seven years. An operational SCIAMACHY/GEO ray-matching technique was presented, along with enhancements to improve radiance pair sampling. These enhancements did not bias the underlying intercalibration and provided enough sampling to allow up to monthly monitoring of the GEO sensor degradation. The results of the SCIAMACHY/GEO intercalibration were compared with other operational four-year Meteosat-9 0.65-μm calibration coefficients and were found to be within 1% of the gain, and more importantly, it had one of the lowest temporal standard errors of all the methods. This is more than likely that the GEO spectral response function could be directly applied to the SCIAMACHY radiances, whereas the other operational methods inferred a spectral correction factor. This method allows the validation of the spectral corrections required by other methods.**

***Index Terms*—Geostationary visible imager calibration, Scanning Imaging Absorption Spectrometer for Atmospheric Cartography (SCIAMACHY), spectral band adjustment factor (SBAF).**

Manuscript received February 29, 2012; revised July 13, 2012 and September 13, 2012; accepted October 29, 2012. Date of publication January 21, 2013; date of current version February 21, 2013. This work was supported in part by the National Aeronautics and Space Administration Earth Science Enterprise Office through the Climate Absolute Radiance and Refractivity Observatory, Clouds and the Earth's Radiant Energy System, the Satellite Calibration Interconsistency Programs and in part by the National Atmospheric and Oceanic Administration through the Climate Data Records Program under Grant MOA IA1-1016.

D. R. Doelling, C. Lukashin, and P. Minnis are with the Climate Sciences Branch, NASA Langley Research Center, Hampton, VA 23681 USA (e-mail: david.r.doelling@nasa.gov; constantine.lukashin-1@nasa.gov; p.minnis@nasa.gov).

B. R. Scarino, D. Morstad, A. Gopalan, and R. Bhatt are with the Science Systems and Applications, Inc., Hampton, VA 23666 USA (e-mail: Benjamin.r.scarino@nasa.gov; Daniel.morstad@nasa.gov; arun.gopalan-1@nasa.gov; Rajendra.Bhatt@nasa.gov).

Color versions of one or more of the figures in this paper are available online at http://ieeexplore.ieee.org.

Digital Object Identifier 10.1109/TGRS.2012.2227760

I. Introduction

THE goal of the Global Space-Based Inter-Calibration System (GSICS) is to provide consistent calibration coefficients across space-based sensors, which are based on best practices that are tied to an absolute calibration reference to provide climate-quality observations [1]. The GSICS effort utilizes either Infrared Atmospheric Sounding Interferometer (IASI) or Atmospheric Infrared Sounder (AIRS) hyperspectral radiances as the calibration reference to calibrate geostationary infrared (IR) imagers (henceforth, geostationary Earth-observing sensors will be abbreviated as GEO). These instruments are used because the hyperspectral radiances are well calibrated and can easily account for spectral response function (SRF) differences [2]–[4]. The difference in calibration between IASI and AIRS is less than 0.1 K across the GEO IR bands [4], suggesting that both are well calibrated and can be used as calibration standards.

To date, no such hyperspectral instrument has been used directly as a GEO visible calibration reference. The calibration of a contemporary well-calibrated visible sensor, such as the MODerate resolution Imaging Spectroradiometer (MODIS), can be transferred to a GEO, which has no onboard calibration, by using bore-sighted, or ray-matched, radiances [5]. However, this calibration approach requires a spectral band adjustment factor (SBAF) to account for the sensor SRF differences. Using hyperspectral Hyperion visible radiances with a 10-nm spectral resolution, Chander *et al.* [6] determined that the SBAF differed by $\sim$5% between the comparable Landsat-7 enhanced thematic mapper and MODIS 0.65-μm bands. Using Scanning Imaging Absorption Spectrometer for Atmospheric Cartography (SCIAMACHY) spectral data in a simulation, Doelling *et al.* [7] found an ocean–land calibration difference of 4.5% between the MODIS and Geostationary Operational Environmental Satellite (GOES-12) visible channels if the sensor spectral bands were not properly taken into account.

Current and historical visible hyperspectral trace-gas monitoring instruments have been of limited use to the calibration community owing to their limited spectral bandwidth and poor spatial resolution. The Backscattered Ultraviolet (BUV), Solar BUV, and Total Ozone Mapping Spectrometer and Ozone Monitoring Instrument instruments have been flown on the Nimbus, National Atmospheric and Oceanic Administration, and Aura satellites since 1970 but are limited spectrally to wavelengths shorter than 0.5 μm. To increase the number

of trace gases that could be measured, the Global Ozone Monitoring Experiment (GOME) was launched in April 1995 on board the European Remote Sensing-2 spacecraft. The GOME 40 $\times$ 320 km footprint has a swath width of 960 km and a spectral resolution of 0.2–0.4 nm between 0.24 and 0.79 μm and was calibrated using a solar diffuser [9]. The advanced GOME-2 instrument on board the MetOp-A satellite, operational since 2006, has a reduced footprint size of 80 $\times$ 40 km and a swath width of 1920 km, with the same spectral range as that of GOME. The SCIAMACHY flies aboard the ENVIronmental SATellite (ENVISAT), launched in 2002. SCIAMACHY operates in the wavelength range from 0.214 to 2.386 μm, with a spectral resolution from 0.22 to 1.48 μm depending on the instrument channel. SCIAMACHY has a nominal nadir footprint of 30 km (along track) $\times$ 60 km (across track) with a full swath of 960 km. However, the across-track sampling depends on the selected spectral cluster (channel) [10]–[12].

The land-observing community has developed many hyperspectral instruments designed for geology and land-use science. These instruments have very high spatial resolution, usually in meters, with limited temporal and spatial coverage. For example, the United States Geological Survey Hyperion sensor on board the Earth Observing satellite samples a 7.5 $\times$ 100 km image at 30 m with a 10-nm spectral resolution between 400 and 2500 nm. However, it does not scan continuously, and the imagery must be ordered in advance, thereby severely limiting its use as a calibration reference sensor.

The future Climate Absolute Radiance and Refractivity Observatory (CLARREO) mission goal is to provide climate-benchmarking measurements, with a focus on improving instrument calibration accuracy [8]. It will also provide highly accurate hyperspectral visible and IR radiances for intercalibration, thus allowing contemporary sensors to provide the science community climate-quality observations. It is expected that GSICS will use the CLARREO reflective solar (RS) hyperspectral sensor to accomplish its calibration goals. CLARREO RS will have a high spatial resolution of 0.5 $\times$ 0.5 km with a swath of 100 km (nadir). For calibration and intercalibration purposes, CLARREO will be required to be capable of 2-D pointing (with gimbal or spacecraft). The spectral resolution will be moderate, at about 4 nm and with a spectral range from 0.32 to 2.3 μm.

The objective of this study is to determine whether it is feasible to directly calibrate a GEO sensor with a contemporary hyperspectral visible instrument in its current operational scan mode. This study will benefit the GSICS and CLARREO visible calibration communities as well as other satellite imager calibration efforts. In the event that a well-calibrated hyperspectral instrument is launched, the methodology of hyperspectral intercalibration will have been established. Although the GOME-2 could serve as a reasonable candidate, the SCIAMACHY instrument has been chosen for this study because it has the greatest spectral range and most closely resembles the characteristics of the future CLARREO instrument.

This paper is outlined as follows. The first step is to verify the calibration accuracy of SCIAMACHY. The GSICS community has recommended that Aqua MODIS be used as the calibration reference until superseded by a superiorly calibrated instrument. Aqua MODIS is temporally more stable than Terra MODIS and is also a better characterized instrument [13]. Section II will compare the calibration of SCIAMACHY to Aqua-MODIS 0.65-μm channel using nearly simultaneous nadir overpass (SNO) (NSNO) measurements. Section III describes three SCIAMACHY/GEO ray-matching radiance pair intercalibration techniques designed to transfer the SCIAMACHY calibration to the GEO visible channels. The precise ray-match technique defines a narrow ray-matching cone to reduce the impact of angular mismatches. The approximate ray-match technique broadens the ray-matching cone and, when compared with the precise technique, is shown to not introduce any biases in the SCIAMACHY/GEO regression, yet it increases the number of radiance pairs. A method of using limited SCIAMACHY spectra with spatial resolution at nadir of 30 $\times$ 60 km is described. This approach allows the significant increase in matched data sampling. Section IV validates the SCIAMACHY/GEO intercalibration. An operational SCIAMACHY/GEO intercalibration method is presented and is compared with other conventional operational methods, such as deserts, deep convective clouds (DCC), and Terra- and Aqua-MODIS/GEO ray matching. Section V contains the conclusions of this paper.

The ray-matching technique [5] transfers the calibration of the reference sensor to the target sensor using reference and target coincident radiance pairs that are bore sighted, where the viewing and solar geometry is very close. These radiance pairs are then linearly regressed to derive the target calibration coefficients based on the reference sensor calibration, where a SBAF has been applied to the reference sensor radiances as if it had the SRF of the target sensor. The SBAFs used in this study were computed from hyperspectral SCIAMACHY radiances convolved with both the reference and the target sensor SRF to derive pseudoreference and target radiance pairs over the intercalibration or invariant Earth target domain. This allows for spectral modeling of the target radiance as a function of the reference radiance. The ray-matching intercalibration approach relies on the calibration accuracy and stability of the reference sensor and is referred to as an intercalibration approach to differentiate the calibration based on the satellite instrument or an invariant target. The reference/target (satellite) intercalibration convention is used in this paper.

II. SCIAMACHY/Aqua-MODIS NSNO Calibration Comparison

SCIAMACHY is on board the ENVISAT, which was launched in March 2002 into a 10:00 local equator crossing time (LECT) sun-synchronous orbit maintained at an 800-km altitude with a 35-day orbit repeat cycle. We used the SCIAMACHY Level-1B data product (SCI_NL_1P, version 7.03) [14] to obtain spectral radiances from 0.24 to 1.75 μm. For this purpose, we have processed the Level-1B data produced with the European Space Agency (ESA)-distributed data calibrator and extracted SCIAMACHY measurements from channels 1 to 6 (all-cal switch) and daily measured (D0) solar irradiance. With these data processing options, the instrument spatial

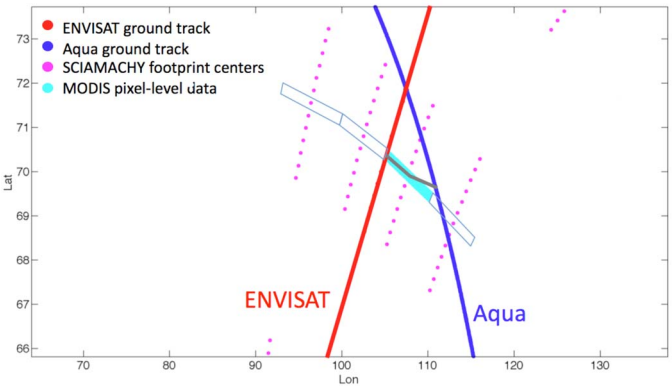

Fig. 1. Illustration of ENVISAT and Aqua ground tracks and accompanying SCIAMACHY footprint centers. The NSNO SCIAMACHY footprint identified with this method is shaded in cyan. The gray lines show the cross-track orientation of the SCIAMACHY footprint and Aqua-MODIS pixels.

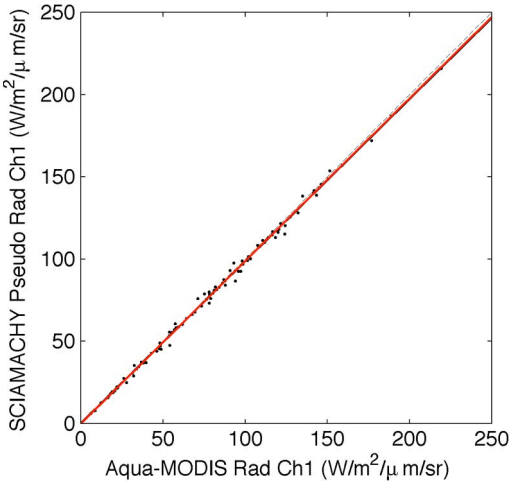

Fig. 2. July 2010 regression scatter plot of the convolved SCIAMACHY radiances (with the MODIS 0.65-μm SRF) against the mean Aqua-MODIS radiance of all pixels contained within the SCIAMACHY footprint. Both the (blue line) linear regression and (red line) force fit are shown, although they are nearly identical. The dotted line represents the diagonal.

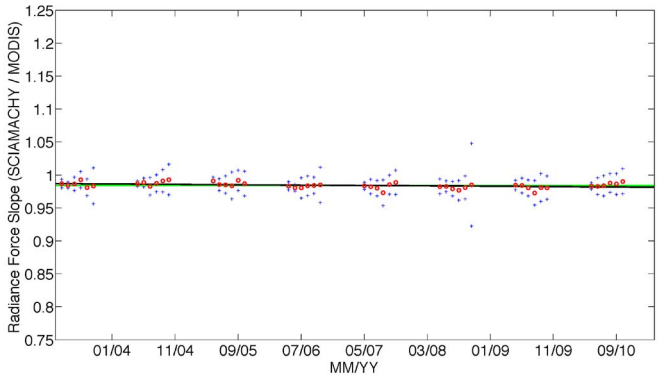

Fig. 3. Monthly Aqua-MODIS-to-SCIAMACHY correction factors from 2003 to 2010 shown in red dots. The monthly standard errors are shown as blue crosses about the means. The black line represents the linear temporal trend. The green line represents the eight-year mean SCIAMACHY/Aqua-MODIS band 1 radiance ratio of 0.9844.

sampling consists of four contiguous footprints with the size of about 30 $\times$ 240 km (nadir). The absolute error estimated for spectral reflectance varies from 2% (channel 4, 595 to 812 nm) to 6% (channel 6, 785 to 1050 nm) [14]. The SCIAMACHY instrument alternates between nadir and limb scan modes every 7 min in order to evenly sample the same atmosphere from both perspectives. Only the nadir scan is utilized in this study. A solar diffuser provides the temporal calibration stability.

The Aqua-MODIS Collection 5 Level 1b Band 1 (0.65 μm) pixel-level radiances, with a nominal resolution of 1 km, were subsampled at 2 km by utilizing every other line and element. The Aqua-MODIS Band 1 ground-to-orbit absolute calibration accuracy in reflectance is $\sim$2% [15], and the temporal calibration relies on the solar diffuser, which is estimated to be stable within 0.5% per decade [13]. Aqua was launched on May 4, 2002 into a 13:30 LECT sun-synchronous orbit at an altitude of 705 km with a 16-day orbit repeat cycle.

Aqua and ENVISAT ground track intersects were predicted from the two-line North American Aerospace Defense elements, which are updated daily. The ground track intersects occur 14 times daily at 71°N latitude at 11:45 local time, thereby assuring near symmetric solar conditions. Because none of the SCIAMACHY nadir footprints straddle the ground track, exact SNOs are not possible with MODIS. The SCIAMACHY footprint is oriented with the major axis (240 km) along the cross track and the minor axis (30 km) along the ground track, with two footprints on either sides of the ground track as shown in Fig. 1. Furthermore, the SCIAMACHY and MODIS cross-track orientations are not parallel. The SCIAMACHY footprint width of 240 km constitutes a range of MODIS pixel-level viewing angles between 0° and 15°. To take advantage of the solar symmetry along the longitude of the ground track intersect, ensuring azimuthal matches, the SCIAMACHY footprint would be optimally bordered between the ground tracks either north or south of the intersect. The southern location was chosen because it has a lower solar zenith angle (SZA) and a better signal-to-noise ratio and there were sufficient samples without including the northern location. Given that the footprints used in this comparison are not exactly at nadir, they are referred to as NSNOs. The mean viewing zenith angle (VZA) for SCIAMACHY and MODIS is 7.5° and 9.8°, respectively. Usually, $\sim$100 NSNO footprints are captured monthly. The number of available Earth view footprints is limited due to the SCIAMACHY limb/nadir duty cycle. To maintain a significant signal-to-noise ratio, only footprints with a SZA less than 70° were used, thus limiting the comparison seasonally from April to September.

All $\sim$1300 MODIS 2-km pixel-level radiances that were located within the domain of the designated SCIAMACHY footprint were averaged and regressed on a monthly basis against the associated SCIAMACHY radiance convolved with the MODIS 0.65-μm SRF. The mean MODIS radiance was normalized to the SZA of the SCIAMACHY footprint. A force-fit regression through the origin is performed to acquire the monthly correction factor. The force fit assumes that the space offset is performed more frequently than the solar look and is accurately known for each instrument. Fig. 2 displays the July 2010 scatter plot. The standard error of the matched SCIAMACHY/MODIS radiance pairs was 2.8%, and the resulting SCIAMACHY/MODIS correction factor is 0.988, thus indicating that SCIAMACHY is biased 1.2% darker than MODIS. This

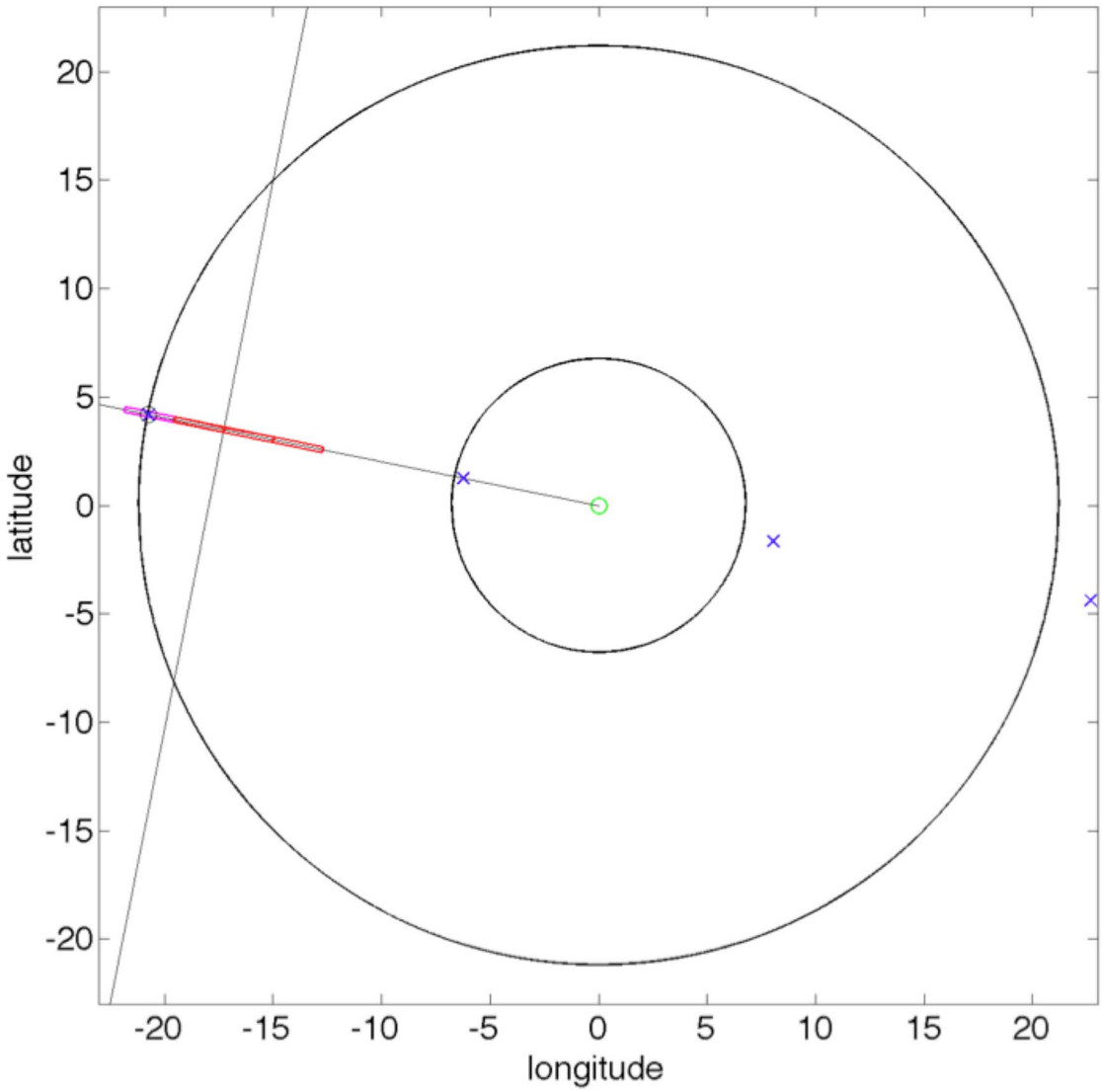

Fig. 4. Illustration of the (blue x) four locations used to match SCIAMACHY 240 km by 30 km footprint centers. The ENVISAT ground track is the nearly vertical line. The four SCIAMACHY cross-track footprints are shown in red. The purple footprint is SCIAMACHY/GEO ray-matched footprint. (Green circle) Meteosat-9 subsatellite point. The inner (outer) circle demarcates the 7.5° (25°) view angle.

difference is well within the 0.65-μm-band uncertainty of 2% absolute calibration accuracy of both instruments [14], [15].

Fig. 3 displays the monthly correction factors from April 2003 to September 2010. The standard deviation of the 48 monthly factors is 0.44%, with an average correction of 0.9844. The individual monthly standard errors are also shown and reveal an increase in the standard error between April and September. This is likely due to the loss of dynamic range resulting from decreasing bright snow coverage across the 70° latitude zone during the summer months. The relative calibration trend was 0.2% between SCIAMACHY and Aqua MODIS. This analysis was also performed using reflectances rather than radiances, and the reflectance monthly standard deviation was 0.89%, a factor of two greater than using radiances. There is a known issue for the SCI_NL_1P product, version 7.03 (ESA announcement in December 2011). Some data were processed with incorrect solar irradiance measurements. The high stability implies that the SCIAMACHY radiance calibration is comparable to the Aqua-MODIS radiance calibration and can be used as a reference to calibrate other operational visible imagers. All GEO calibrations used in this study also use the Aqua-MODIS radiance calibration as a reference.

III. SCIAMACHY/GEO Ray-Match Intercalibration

A. Precise Ray Matching

The four cross-track SCIAMACHY footprints allow only four collocations (blue x's in Fig. 4) over the GEO domain where ray matching, or bore sighting, is possible. Fig. 4 illustrates the orientation of the SCIAMACHY footprints along the ENVISAT ground track for the ray-matched footprint on the far west side, which is shown in purple. This approach matches the GEO VZA with the center SCIAMACHY footprint VZA. The GEO VZA range across the footprint is $\sim 2°$, whereas for SCIAMACHY, it is $\sim 15°$. Because the line that defines

the cross track intersects the GEO subsatellite point, a nearly exact solar and azimuthal geometry match between the two instruments is ensured.

Any time the appropriate SCIAMACHY footprint center is within 40 km (precise ray matching) of one of the four *a priori* SCIAMACHY/GEO colocations, an average is computed using the GEO radiances contained inside the SCIAMACHY footprint. The corresponding SCIAMACHY footprint hyperspectral radiances convolved with the GEO SRF are also computed. Each collocation is usually sampled within 15 min once or twice per month owing to the 35-day ENVISAT ground track repeat cycle. The SCIAMACHY nadir and limb scan-duty cycle reduces the potential matches by half (see [16, Fig. 1]). These cycles equate to less than 40 matches per year. Such few matches cannot possibly resolve the temporal degradation of the GEO visible sensor but serve only to validate postlaunch calibration.

B. Approximate Ray Matching

A strategy to increase the number of ray-matched samples is to broaden the boresight cone diameter. Relaxing the view angle-matching cone allows multiple off-angle matching opportunities for each ground track intersect. Doelling *et al.* [17] demonstrated that the Advanced Very High Resolution Radiometer A.M. and P.M. satellite radiance pair regression slopes based on SNO and off-nadir SNO radiances were rather similar. When two polar orbiters scan in cross-track mode, there are two lines of constant view angle pixels, which cross at the ground track intersect. As long as the view angle is less than 10°, the relative azimuthal angle difference is small along the constant view angle line. The pixels were referred to as the off-nadir SNO radiance pairs. The advantage of off-nadir matches is the increase in radiance pairs, which usually decreases the uncertainty of the radiance pair regression. Minnis *et al.* [5] successfully transferred the calibration from one sensor to another using a ray-match cone within 15° for both view and azimuth angles over a 50-km region. Following that constraint, the ray-match cone radius was extended to 160 km (approximate ray matching), which allows for more ray-matched SCIAMACHY/GEO footprints along the SCIAMACHY ground track. Up to 500 matches per year are possible depending on the GEO imaging schedule, enough to monitor the GEO visible sensor degradation seasonally.

To ensure that approximate ray matching does not introduce any angular mismatch biases compared with precise ray matching, the GEO radiances are first calibrated against Aqua MODIS in order to remove any temporal trends of the GEO sensor. If the SCIAMACHY/GEO radiance pair approximate regression slope is nearly identical with the precise ray-match slope, then the approximate ray matching is still within tolerance and validated. The GEO imager counts were first calibrated against Aqua MODIS using monthly regressed ray-matched radiance pairs [5], [18] over the GEO equatorial domain. A SBAF was applied to the GEO radiance to account for the spectral band difference between the GEO and Aqua-MODIS 0.65-μm visible bands as in [7]. Fig. 5 displays the GEO and Aqua-MODIS SRFs used in this study. The GEO

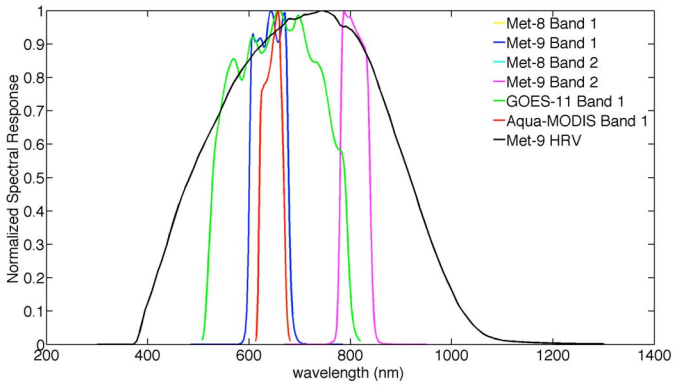

Fig. 5. SRF of the GEO and Aqua-MODIS data sets used in this study. The Meteosat-8 and Meteosat-9 bands are similar. Band 1 is the 0.65-μm channel. Band 2 is the 0.86-μm channel.

4-km nominal resolution imager data used in this study were obtained from man computer interactive data access system area files. The monthly slopes, or gains, were linearly regressed in time to estimate the GEO sensor instrument degradation. The GEO imager visible counts C are converted to radiance L by

$$L = (\Delta g_1 d + g_o)(C - C_o) \tag{1}$$

where g_o is the initial gain, Δg_1 is the linear term of the trend, d denotes the days since launch, and C_o is the offset count. The Aqua-MODIS-based GEO imager intercalibration coefficients used in this study are given in Table I. The associated temporal [18] and SBAF [7] uncertainty of the calibration coefficients is also given.

The temporal uncertainty is the standard error of the linear regression of the monthly GEO gains over the data set time period. The SBAF uncertainty is the standard error of the second-order polynomial regression of the pseudo SCIAMACHY MODIS and GEO SRF convolved radiances from all of the SCIAMACHY footprints over the GEO/MODIS intercalibration domain. The domain is centered at the GEO subsatellite location and bounded by $\pm 20°$ in latitude and $\pm 30°$ in longitude. Only ocean surfaces are included in the domain in order to reduce the spectral impact of the intercalibration. Fig. 6 shows the SCIAMACHY radiances, convolved with the GEO SRFs, against the Meteosat-9 0.65-μm mean footprint radiances during April 2007 through December 2010, along with the respective force-fit regression for both the precise and approximate methods. The number of precise and approximate ray-matched pairs is 169 and 2292, respectively. This is a factor of 13 more approximate ray-matched pairs than precise. Table II shows that, for all the GEO imagers, the approximate and precise force-fit (through the origin) regression slopes are within 0.5%, well within the standard error of the regression of $\sim$4.5%. The only exception is the Meteosat-9 high resolution visible (HRV) band with a slope difference of 1%, which also has the least amount of precise radiance pairs. This confirms that the approximate ray-matched radiances maintain the regression slope and uncertainty of the precise ray match, but with the added benefit of providing an order of magnitude more matches.

TABLE I
AQUA-MODIS/GEO RAY-MATCHED CALIBRATION COEFFICIENTS USED IN THIS STUDY

GEO dataset	g_0 ($Wm^{-2}sr^{-1}\mu m^{-1}$ /count)	Dg_1 ($Wm^{-2}sr^{-1}\mu m^{-1}$ /count/day)	Count offset	dataset time period	Temporal uncertainty (%)	SBAF uncertainty (%)
MET-9 0.65 µm	0.5462	0.057e-4	51	April 2007 to Dec. 2010	0.96	0.28
MET-9 0.86 µm	0.4192	0.070e-4	51	April 2007 to Dec. 2010	1.91	4.85
MET-9 HRV	0.5560	0.067e-4	51	April 2007 to Dec. 2010	0.67	1.42
MET-8 0.65 µm	0.6235	0.107e-4	51	March 2004 to April 2007	0.54	0.31
MET-8 0.86 µm	0.4763	0.044e-4	51	March 2004 to April 2007	1.83	4.85
GOES-11 0.65 µm	0.4838	0.702e-4	29	June 2006 to Dec. 2010	0.86	1.37

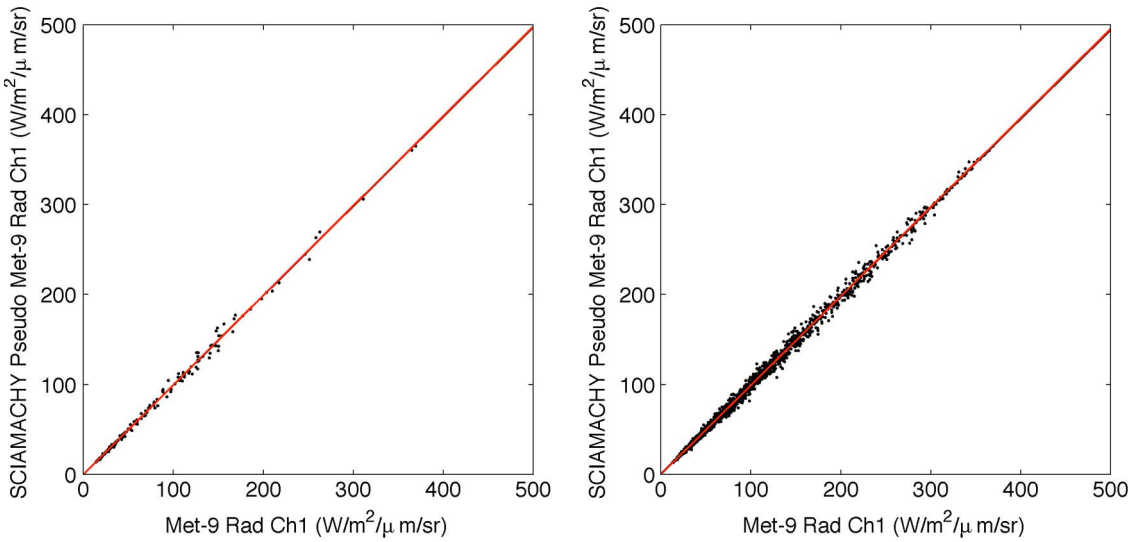

Fig. 6. Regression scatter plot of the convolved SCIAMACHY radiance (with the Meteosat-9 0.65-μm SRF) against the mean Meteosat-9 radiance within the SCIAMACHY footprint during April 2007 to December 2010. Both the (black line) linear regression and (red line) force fit for the (left panel) precise and (right panel) approximate methods are shown.

TABLE II
SCIAMACHY/GEO FORCE-FIT (THROUGH THE ORIGIN) SLOPE AND ASSOCIATED STANDARD ERROR AS A FUNCTION OF GEO SATELLITE DATA SET. BOTH THE PRECISE AND APPROXIMATE VALUES ARE GIVEN AS (PRECISE/APPROXIMATE) IN EACH COLUMN. THE FIRST GEO DATA SET IS BASED ON SPECTRAL CLUSTER #24

GEO Dataset	#	SCIAMACHY/GEO 0.65µm force fit	Standard error (%)
Met-9 Cluster #24	502/7401	0.993/0.991	4.5/5.1
Met-9 0.65 µm	169/2292	0.996/0.991	4.7/4.1
Met-9 0.86 µm	158/2212	0.983/0.978	4.4/4.0
Met-9 HRV	76/1082	0.998/0.988	5.9/5.0
Met-8 0.65 µm	114/1641	0.983/0.988	4.9/4.4
Met-8 0.86 µm	114/1641	0.999/1.004	4.5/4.2
GOES-11 0.65 µm	84/1315	0.990/0.992	4.7/6.2

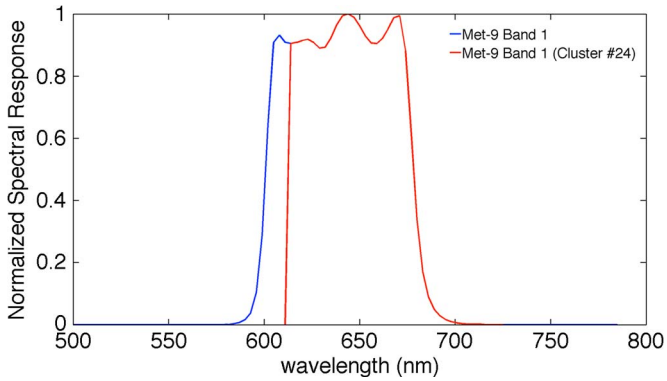

Fig. 7. Meteosat-9 band 1 (0.65 μm) SRF (red line) within the spectral range of the spectral cluster #24 and (blue line) out of range.

C. Limited Spectral Cluster Ray Matching

The SCIAMACHY nadir spectrum is divided into 56 wavelength clusters, each with their own integration time. The integration time determines the cluster footprint spatial resolution. Wavelengths important for trace-gas studies are assigned the highest spatial resolution [19]. Cluster #24 has a spectral range of 0.613 to 0.726 μm at a 0.48-nm spectral resolution and was extracted and calibrated using SCIAMACHY processing software. The SCIAMACHY footprint corresponding to spectral cluster #24 is 30 $\times$ 60 km, with a swath width of 960 km. The Meteosat-9 0.65-μm bandwidth is between the same spectral bounds as mentioned earlier, except for a small portion of out-of-band response as shown in Fig. 7. To account for the missing energy not seen by SCIAMACHY cluster #24, a lost energy

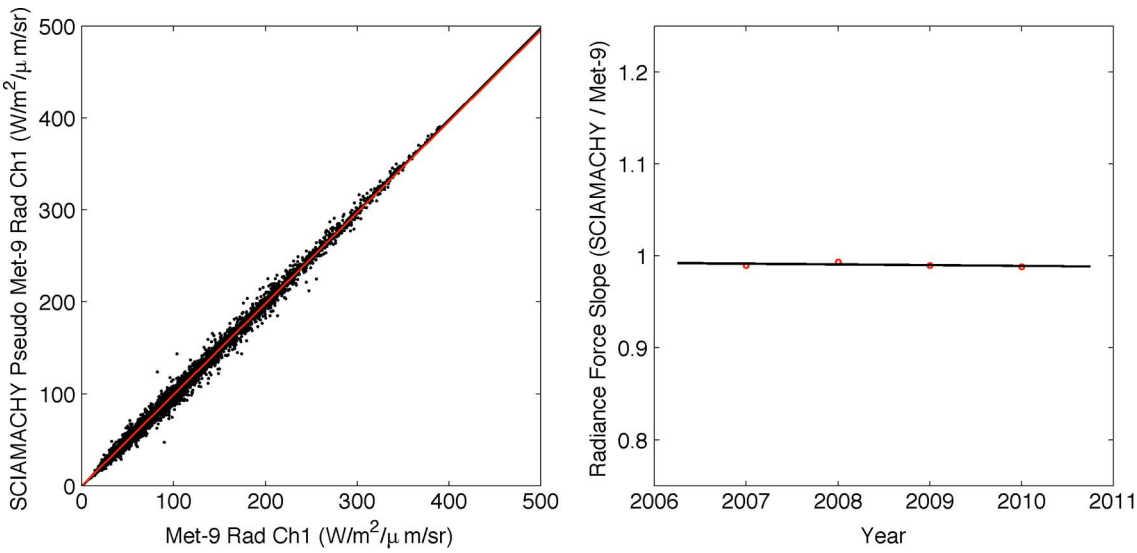

Fig. 8. (Left panel) Regression scatter plot of the convolved SCIAMACHY radiance (with the Meteosat-9 0.65-μm SRF) against the mean Meteosat-9 radiance within the SCIAMACHY *cluster* footprint during April 2007 to December 2010. Both the (black line) linear regression and (red line) force fit are shown. (Right panel) Annual Meteosat-9 0.65-μm to SCIAMACHY radiance correction factors between 2007 and 2011, shown with red circles.

adjustment factor (LEAF) is applied to the Meteosat-9 radiance values. The LEAF is derived by averaging all of the 30×240 km footprint convolved radiances for the limited Meteosat-9 SRF (contained within the spectra of cluster #24) divided by the full Meteosat-9 SRF convolved radiances. Footprints from April 2007 through December 2010 are used to derive the LEAF, which was found to have a value of 0.96.

Fig. 8 (left panel) displays the SCIAMACHY-approximate-cluster-derived Meteosat-9-SRF-convolved radiances paired with the cluster-domain-averaged Meteosat-9 pixel-level radiances. Table II displays the associated regression statistics. The precise and approximate cluster force-fit slope is 0.2%, ensuring that no angular biases are introduced using the approximate cluster method. The approximate cluster and large-footprint force fits are nearly identical, indicating that the LEAF accurately predicted the missing energy not captured by the cluster spectrum. The cluster standard error, however, is 5.1%, which is greater than the approximate standard error of 4.1%. The LEAF on average corrected the radiances, but because it is a single value, it adds noise to the regression. Nevertheless, the cluster footprint has the advantage of having improved ray-matching conditions, i.e., the SCIAMACHY VZA range is 4°, rather than 15° for the full footprint.

IV. SCIAMACHY/GEO Intercalibration Validation

If SCIAMACHY was perfectly calibrated against both Aqua MODIS and GEO, where GEO was calibrated perfectly with Aqua MODIS, then the ratio of the two intercalibrations should equal 1.0. This validation will confirm that the SCIAMACHY/GEO intercalibration approach is robust if the calibration ratio is within the uncertainty of the individual satellite pair intercalibrations. The calibration validation relationship is

$$ratio = \frac{SCIA}{GEO} * \frac{Aqua}{SCIA} \tag{2}$$

where the y-axis variable in the radiance pair plot is indicated in the numerator of the ratio. Using the SCIA/GEO approximate force fit from Fig. 6(b) for the Meteosat-9 0.65-μm band and the value of Aqua/SCIA, which is the inverse of the Aqua-to-SCIAMACHY correction factor from Fig. 3, (2) yields the ratio of $1.007 = 0.991 * [1/0.9844]$. If the intercalibration was perfect, the ratio would equal 1.00, and thus, the mean bias error is 0.7%.

To place the bias in proper context, it is necessary to consider the uncertainty in the estimate. The total uncertainty is the square root of the sum of the squares of the uncertainties of the individual terms. The standard error of the temporal linear regression of the monthly slopes provides an estimate of the uncertainty. The uncertainty of the Aqua/SCIA correction factor is equal to the monthly standard deviation of 0.44% in Fig. 3. The SCIAMACHY/GEO uncertainty is the standard deviation of the annual regression force slopes based on the approximate radiance pair matches as shown in Fig. 8 (right panel). The annual cluster force fits have a standard deviation of 0.42%. The Aqua/GEO uncertainties used to determine the GEO calibration are based on the calibration coefficients in Table I, as derived following the approach using the temporal trend of monthly calibration coefficients as in [18]. For Meteosat-9, the Aqua/GEO uncertainty is 0.96%. Thus, the total uncertainty is 1.11%, indicating that the 0.7% bias in the three-way validation is statistically no different from a 0.0% bias.

Table III lists the validation slopes and associated uncertainties with and without the SBAF uncertainty for all the GEO imagers evaluated in this study. All of the validation slopes are within their respective uncertainties without using SBAF, thus validating the SCIAMACHY/GEO intercalibration approach. This indicates the SCIAMACHY/GEO intercalibration methodology is robust for nearly all cases. The only exception is the Meteosat-8 0.86-μm band. The large uncertainties associated with the 0.86-μm and HRV nearly broad-band channels, which reside in the near IR wavelengths, are primarily due to the larger uncertainty of the SBAFs. These results validate

TABLE III
CALIBRATION VALIDATION TABLE. EQUATION (2) DEFINES THE RATIO. THE VALIDATION TOTAL UNCERTAINTY IS BASED ON ALL THE INDIVIDUAL TEMPORAL UNCERTAINTIES. UNDER THE VALIDATION TOTAL COLUMN, THE LEFT UNCERTAINTY IS COMPUTED WITHOUT SBAF, AND THE RIGHT IS COMPUTED WITH SBAF. THE FIRST GEO DATA SET IS BASED ON SPECTRAL CLUSTER #24

GEO dataset	SCIA/GEO		SCIA/Aqua		Validation	
	slope	(%)	slope	(%)	ratio	Total (%)
MET-9 Cluster #24	0.991	0.42	0.984	0.44	1.007	1.14/1.17
MET-9 0.65μm	0.991	0.35	0.984	0.44	1.007	1.11/1.14
Met-9 0.86μm	0.978	0.57	0.984	0.44	0.994	2.04/5.26
Met-9 HRV	0.988	0.78	0.984	0.44	1.004	1.12/1.81
MET-8 0.65μm	0.988	0.46	0.984	0.44	1.004	0.83/0.89
Met-8 0.86μm	1.004	0.49	0.984	0.44	1.020	1.94/5.23
GOES-11 0.65μm	0.993	0.72	0.984	0.44	1.009	1.20/1.82

the use of the SBAF in deriving the Aqua-MODIS/GEO ray-matched intercalibration coefficients.

A. Operational SCIAMACHY/GEO Intercalibration Validation

Two SCIAMACHY/GEO intercalibration methods are capable of monitoring the GEO degradation, the approximate and the cluster ray-match technique. The SCIAMACHY/Meteosat-9 approximate ray match provides ∼150 radiance pairs every three months. The number of cluster radiance pairs is ∼170 per month. On a monthly or quarterly basis, the SCIAMACHY convolved Meteosat-9 SRF radiances were regressed using a force fit through zero against the average Meteosat-9 pixel-level raw counts, after subtracting off the space count of 51, within the SCIAMACHY footprint. The SCIAMACHY radiances were also scaled to the Aqua reference calibration by dividing the SCIAMACHY radiances by 0.9844 (see Fig. 2). Fig. 9 shows the linear regression of the monthly approximate (labeled Large in Fig. 9) and cluster force-fit slopes. The standard errors are 0.56% and 0.52% for the approximate and cluster methods, respectively. Both methods had a four-year average identical gain of 0.556.

Fig. 9 also includes results from the Terra- and Aqua-MODIS/GEO ray matching, DCC, and Libyan Desert operational calibration procedures [18] for comparison with the SCIAMACHY/GEO intercalibrations. All of the procedures used Aqua MODIS as the calibration reference, and each procedure provides both temporal sensor degradation monitoring and absolute calibration transfer based on the reference sensor. Terra MODIS was radiometrically scaled to Aqua MODIS based on [13]. The average Meteosat-9 four-year gains and temporal standard errors are listed in Fig. 9 for all of the methods. The four-year average gains are within 1% for all six methods, verifying that, statistically, the SCIAMACHY radiances are anchored temporally to the Aqua-MODIS radiance calibration. The SCIAMACHY/GEO intercalibration provides one of the lowest temporal uncertainties of all methods, which was anticipated, given that this method accounts for the GEO SRF differences. Also, the SCIAMACHY/GEO intercalibration offers the opportunity to validate the SBAFs within an uncertainty of ∼0.5%.

V. CONCLUSION

This study examines the feasibility of using SCIAMACHY large-footprint (30 km by 240 km) hyperspectral radiances

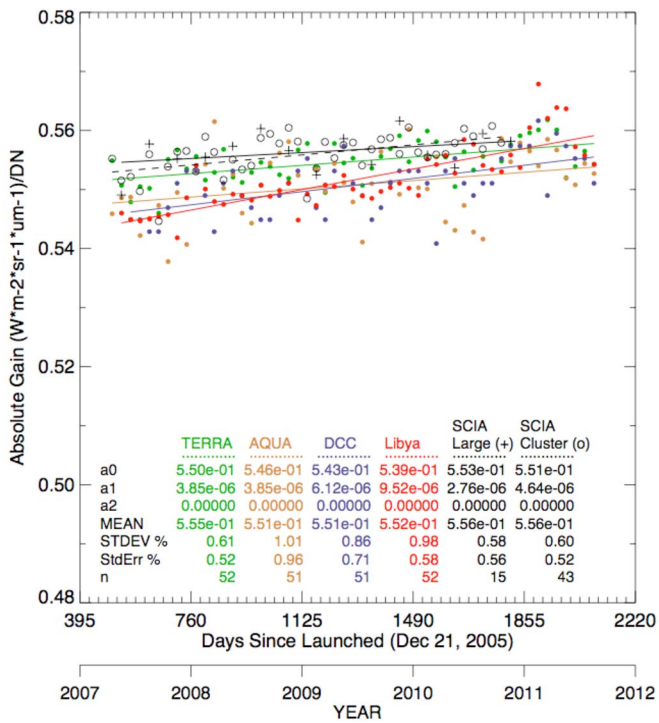

Fig. 9. Meteosat-9 10-b count calibration gains derived from various methods described in the text. The approximate large-footprint and approximate cluster SCIAMACHY methods are labeled as Large and Cluster, respectively. All calibration gains, including SCIAMACHY, use Aqua-MODIS band 1 as a reference.

to intercalibrate GEO visible sensors. The SCIAMACHY/GEO intercalibration technique will benefit the GSICS and CLARREO visible calibration communities because, in the event that a hyperspectral sensor dedicated to calibration becomes available, a validated technique will already be in place.

The temporal stability of SCIAMACHY was evaluated against the calibration of Aqua-MODIS 0.65-μm using NSNOs. It was found that the SCIAMACHY/Aqua-MODIS monthly correction factors are within 0.44% with an associated temporal trend of -0.2% per decade. The excellent agreement is due to the fact that both sensors use the sun to monitor their degradation. It was shown that SCIAMACHY can be used as calibration reference, and thus, a SCIAMACHY/GEO ray-match intercalibration technique was presented. Precise SCIAMACHY/GEO ray matching resulted in few sampled radiance pairs. The approximate ray-matching method allowed for more radiance pairs over the lifetime of the satellite by increasing the boresight cone diameter. It was found that the calibration gain difference between the methods is ∼0.5%, thus assuring that the approximate ray-matched radiances did not bias the calibration.

The technique was also applied to the smaller SCIAMACHY cluster (30 × 60 km) limited spectra footprints. A LEAF was applied to account for the reduced portion of the Meteosat-9 SRF that was contained within the cluster spectral range. The cluster technique provided enough radiance pairs such that they could then be regressed monthly in order to monitor the GEO calibration.

The approximate SCIAMACHY/GEO intercalibration was validated against the ratio of the Aqua-MODIS/GEO and

SCIAMACHY/Aqua-MODIS intercalibrations. The three-way calibration validation indicated that the SCIAMACHY/GEO intercalibration was within the uncertainty based on the individual calibration uncertainties and thereby validated the technique. The standard deviation of the approximate cluster monthly Meteosat-9 0.65-μm monthly calibration gains over four years is 0.51%, with a temporal trend of +1.7% per decade. The corresponding approximate large-footprint three-monthly standard deviation is 0.58%, with a temporal trend of 1.0% per decade. This excellent agreement validates the SCIAMACHY-cluster/GEO intercalibration technique. The Meteosat-9 0.65-μm SCIAMACHY/GEO intercalibration was compared with the Terra-MODIS, Aqua-MODIS ray-matching, deep convective cloud, and Libyan Desert calibration methods. The SCIAMACHY/GEO intercalibration was within 1% of these other techniques and had one of the lowest temporal standard errors of all methods. This technique allows the opportunity to validate the Aqua-MODIS/GEO 0.65-μm SBAF to improve upon the Terra- and Aqua-MODIS/GEO ray-matching techniques.

ACKNOWLEDGMENT

The authors would like to thank J. Xiong and the MODIS team for the assistance with the MODIS data. The MODIS data were obtained from the NASA Langley Distributed Active Archive Center. This study could not have been completed without the Scanning Imaging Absorption Spectrometer for Atmospheric Cartography (SCIAMACHY) data provided by the European Space Agency ENVISAT program. The authors would like to thank J. Burrows, S. Noel, and K. Bramstedt at Bremen University and R. Snel at the Netherlands Institute for Space Research for the assistance with the SCIAMACHY data. The GEO satellite data were obtained from the University of Wisconsin Space Science and Engineering Center, Madison, WI.

REFERENCES

[1] M. Goldberg, G. Ohring, J. Butler, C. Cao, R. Datla, D. Doelling, V. Gärtner, T. Hewison, B. Iacovazzi, D. Kim, T. Kurino, J. Lafeuille, P. Minnis, D. Renaut, J. Schmetz, D. Tobin, L. Wang, F. Weng, X. Wu, F. Yu, P. Zhang, and T. Zhu, "The Global Space-based Inter-Calibration System (GSICS)," *Bull. Amer. Meteorol. Soc.*, vol. 92, no. 4, pp. 467–475, Apr. 2011.

[2] X. Wu and F. Yu, GSICS Algorithm Theoretical Basis Document (ATBD) for GOES-AIRS/IASI Inter-Calibration. Draft version dated 2009. [Online]. Available: https://gsics.nesdis.noaa.gov/wiki/Development/AtbdCentral

[3] M. M. Gunshor, T. J. Schmit, W. P. Menzel, and D. C. Tobin, "Intercalibration of broadband geostationary imagers using AIRS," *J. Atmos. Ocean. Technol.*, vol. 26, no. 4, pp. 746–758, Apr. 2009.

[4] L. Wang, X. Wu, M. Goldberg, C. Cao, Y. Li, and S.-H. Sohn, "Comparison of AIRS and IASI radiances using GOES imagers as transfer radiometers toward climate data records," *J. Appl. Meteorol. Climatol.*, vol. 49, no. 3, pp. 478–492, Mar. 2010.

[5] P. Minnis, L. Nguyen, D. R. Doelling, D. F. Young, and W. Miller, "Rapid calibration of operational and research meteorological satellite imagers. Part I: Evaluation of research satellite visible channels as references," *J. Atmos. Ocean. Technol.*, vol. 19, no. 9, pp. 1233–1249, Sep. 2002.

[6] G. Chander, N. Mishra, D. L. Helder, D. Aaron, T. Choi, A. Angal, and X. Xiong, "Use of EO-1 Hyperion data to calculate spectral band adjustment factors (SBAF) between the L7 ETM+ and Terra MODIS sensors," in *Proc. IEEE IGARSS*, Jul. 25–30, 2010, pp. 1667–1670.

[7] D. R. Doelling, C. Lukashin, P. Minnis, B. Scarino, and D. Morstad, "Spectral reflectance corrections for satellite intercalibrations using SCIAMACHY data," *IEEE Geosci. Remote Sens. Lett.*, vol. 9, no. 1, pp. 119–123, Jan. 2012.

[8] Space Studies Board, National Research Council, "Earth science and applications from space: National imperatives for the next decade and beyond," in *Decadal Survey*. Washington, DC: National Academy Press, 2007.

[9] J. P. Burrows, M. Weber, M. Buchwitz, V. Rozanov, A. Ladstätter-Weißenmayer, A. Richter, R. DeBeek, R. Hoogen, K. Bramstedt, K.-U. Eichmann, M. Eisinger, and D. Perner, "The Global Ozone Monitoring Experiment (GOME): Mission concept and first scientific results," *J. Atmos. Sci.*, vol. 56, no. 2, pp. 151–175, Jan. 1999.

[10] H. Bovensmann, J. P. Burrows, M. Buchwitz, J. Frerick, S. Noël, V. V. Rosanov, K. V. Chance, and A. P. H. Goedec, "SCIAMACHY: Mission objectives and measurement modes," *J. Atmos. Sci.*, vol. 56, no. 2, pp. 127–150, Jan. 1999.

[11] J. Skupin, S. Noël, M. W. Wuttke, M. Gottwald, H. Bovensmann, M. Weber, and J. P. Burrows, "SCIAMACHY solar irradiance observation in the spectral range from 240 to 2380 nm," *Adv. Space Res.*, vol. 35, no. 3, pp. 370–375, 2005.

[12] G. Lichtenberg, Q. Kleipool, J. M. Krijger, G. van Soest, R. van Hees, L. G. Tilstra, J. R. Acarreta, I. Aben, B. Ahlers, H. Bovensman, K. Chance, A. M. S. Gloudemans, R. W. M. Hoogeveen, R. T. N. Jongma, S. Noël, A. Piters, H. Schrijver, C. Schrijvers, C. E. Sioris, J. Skupin, S. Slijkhuis, P. Stammes, and M. Wuttke, "SCIAMACHY Level 1 data: Calibration concept and in-flight calibration," *Atmos. Chem. Phys.*, vol. 6, no. 12, pp. 5347–5367, Nov. 2006.

[13] A. Wu, X. Xiong, D. R. Doelling, D. L. Morstad, A. Angal, and R. Bhatt, "Characterization of Terra and Aqua MODIS VIS, NIR, and SWIR spectral band calibration stability," *IEEE Trans. Geosci. Remote Sens.*, vol. 51, no. 6, Jun. 2013, to be published. [Online]. Available: http://ieeexplore.ieee.org

[14] Disclaimer for SCIAMACHY IPF 7.03 Level 1b Products (SCI_NL_1P) PO-RS-MDA-GS-2009, vol. 15, no. 3L 2011.

[15] X. Xiong, J. Sun, A. Wu, K. Chiang, J. Esposito, and W. Barnes, "Terra and Aqua MODIS calibration algorithms and uncertainty analysis," in *Proc. SPIE, Sens., Syst., Next-Gen. Satellites IX*, 2005, vol. 5978, p. 597 80V.

[16] J. R. Acarreta and P. Stammes, "Calibration comparison between SCIAMACHY and MERIS onboard ENVISAT," *IEEE Geosci. Remote Sens. Lett.*, vol. 2, no. 1, pp. 31–35, Jan. 2005.

[17] D. R. Doelling, V. Chakrapani, P. Minnis, and L. Nguyen, "The calibration of NOAA-AVHRR visible radiances with VIRS," in *Proc. AMS 11th Conf. Atmos. Radiation*, Madison, WI, Oct. 15–18, 2001, pp. 614–617.

[18] D. L. Morstad, D. R. Doelling, R. Bhatt, and B. Scarino, "The CERES calibration strategy of the geostationary visible channels for CERES cloud and flux products," in *Proc. SPIE*, 2011, vol. 8153, p. 815 316.

[19] L. G. Tilstra and P. Stammes, "Intercomparison of reflectances observed by GOME and SCIAMACHY in the visible wavelength range," *Appl. Opt.*, vol. 45, no. 17, pp. 4129–4135, Jun. 2006.

David R. Doelling received the B.S. degree in meteorology from The University of Utah, Salt Lake City, in 1985 and the M.S. degree in atmospheric science from the University of Washington, Seattle, in 1991.

He is currently a Senior Research Scientist with the National Aeronautics and Space Administration (NASA) Langley Research Center, Hampton, VA, where he is the Time Interpolation and Spatial Averaging Sublead for the Clouds and Earth's Radiant Energy System (CERES) project and responsible for the diurnal averaging and spatial gridding of CERES footprint cloud and radiative flux parameters. He is also a member of the Geostationary Earth Radiation Budget Experiment and Megha-Tropique science teams, projects similar to CERES that measure broad-band fluxes. He has studied the orbital sampling errors for proposed satellites as a member of the Climate Absolute Radiance and Refractivity Observatory science definition team. He is the Global Space-based Inter-Calibration System NASA representative and the lead for geostationary/Moderate Resolution Imaging Spectroradiometer ray-matching and deep convective cloud visible calibration methods. His research interests include geostationary imager calibration, diurnal averaging techniques of satellite observations, and satellite sampling studies.

Benjamin R. Scarino received the M.S. degree in meteorology from the Pennsylvania State University, State College, in 2010.

Shortly thereafter, he was hired by Science Systems and Applications, Inc., Hampton, VA, as a Staff Research Scientist, where he supports the Clouds and the Earth's Radiant Energy System Project, working on cloud and radiation data-set development and on-orbit calibration.

Daniel Morstad received the B.S. and M.S. degrees in electrical engineering from South Dakota State University, Brookings, in 2007 and 2009, respectively. His graduate research focused on the development of a statistically based automation technique for selecting the most temporally invariant Earth targets based on the Landsat-5 Thematic Mapper data record.

He is currently a Research Scientist with Science Systems and Applications, Inc., Hampton, VA, in support of the Clouds and Earth's Radiant Energy System project at the National Aeronautics and Space Administration Langley Research Center, Hampton. He is primarily responsible for maintaining the real-time geostationary visible sensor calibration record and is currently developing a deep convective cloud absolute calibration technique that will be vital to the uniform radiometric calibration of both past and future Earth-observing sensors.

Arun Gopalan received the B.S degree in mechanical engineering from the Victoria Jubilee Technical Institute, University of Bombay, Bombay, India, in 1991 and M.S. degree in mechanical engineering from the State University of New York, Stony Brook, in 1993 and completed all Ph.D. requirements excluding dissertation defense as of 1997 (State University of New York, Stony Brook). His dissertation focused on the research and development of an optimal retrieval algorithm for simultaneous extraction of diurnal stratospheric nitrogen dioxide and aerosol extinction profiles using Earth-limb Infrared Emission measurements from the National Aeronautics and Space Administration (NASA) Upper Atmospheric Research Satellite cryogenic limb array etalon spectrometer instrument.

He is currently a Senior Research Scientist with Science Systems and Applications, Inc., based at Hampton, VA, in support of the NASA Langley Research Center's Cloud and Earth's Radiant Energy System and Climate Absolute Radiance and Refractivity Observatory projects. He has previously coauthored a number of journal papers and worked in the area of satellite remote sensing for over 15 years with earth science research groups at the NASA Goddard Space Flight Center, Greenbelt, MD, and the National Center for Atmospheric Research, Boulder, CO. His research interests include studies of postlaunch calibration techniques to understand satellite sensor performance, science retrieval algorithm development, remotely sensed data processing methods, aerosol-cloud-climate feedback mechanisms, visualization of large-scale Earth science data sets, and data mining.

Rajendra Bhatt received the B.S. degree in electronics engineering from Tribhuvan University, Kirtipur, Kathmandu, Nepal in 2002 and the M.S. degree in electrical engineering from South Dakota State University (SDSU), Brookings, in 2009. At SDSU, he has studied the long-term radiometric stability of and calibrated the Landsat-1 through Landsat-5 multispectral scanner system sensors using pseudoinvariant calibration sites.

He is currently a Research Scientist with Science Systems and Applications, Inc., Hampton, VA, in support of the Clouds and Earth's Radiant Energy System project at the National Aeronautics and Space Administration Langley Research Center in Hampton, where he is developing techniques of in-flight calibration of satellite visible and infrared observations to assess the sensor's performance on orbit and ensure the usability of climate data.

Constantine Lukashin received the M.S. degree in nuclear physics and engineering from Saint Petersburg Polytechnic University, Saint Petersburg, Russia, in 1990 and the Ph.D. degree in physics from Virginia Tech, Blacksburg, in 2000.

He participated in nuclear and high energy particle physics experiments from 1990 to 2001, working at national accelerator facilities in Russia, Italy, and the USA. In 2001, he has joined the National Aeronautics and Space Administration (NASA) Clouds and Earth's Radiant Energy System (CERES) team as a Research Scientist for the development and validation of the angular distribution models (ADMs). As a member of the CERES team, he developed an artificial neural network approach for reproducing ADMs in the absence of coincident imager observations. He is currently a Research Physical Scientist with the NASA Langley Research Center, Hampton, VA, where he is responsible for developing Climate Absolute Radiance and Refractivity Observatory reference intercalibration methodology in the reflected solar wavelength range.

Patrick Minnis is a native of Oklahoma City, OK. He received the B.E. degree in materials science and metallurgical engineering from Vanderbilt University, Nashville, TN, in 1972, the M.S. degree in atmospheric science from Colorado State University, Fort Collins, in 1978, and the Ph.D. degree in meteorology from The University of Utah, Salt Lake City, in 1991.

He is currently a Senior Research Scientist with the Climate Sciences Branch, National Aeronautics and Space Administration (NASA) Langley Research Center, Hampton, VA, where he has served for more than 33 years. His research is focused on the remote sensing of clouds and surface properties from satellite imagery for weather and climate investigations. He is the author/coauthor of over 200 peer-reviewed publications. He is a member of the Clouds and Earth's Radiant Energy System, Atmospheric Radiation Measurement, Cloud-Aerosol Lidar and Infrared Pathfinder Satellite Observation, and Aviation Climate Change Research Initiative Science Teams and leads a research group conducting analyses of polar-orbiting and geostationary satellite data for field missions, aircraft safety, and weather and climate research.

Dr. Minnis is a fellow of the American Geophysical Union and the American Meteorological Society (AMS) and a member of the American Institute of Aeronautics and Astronautics (AIAA). He was the recipient of NASA medals for Exceptional Scientific Achievement in 1993, Exceptional Achievement in 2005, and Exceptional Service in 2008; the AMS Henry G. Houghton Award for Atmospheric Physics in 1998; and the 2011 AIAA Losey Atmospheric Sciences Award.